Journal of Physiology (1991), **440**, *pp.* 601–621
With 10 *figures*
Printed in Great Britain

COMPARISON OF THE SEROTONIN-SENSITIVE AND Ca^{2+}-ACTIVATED K^+ CHANNELS IN *APLYSIA* SENSORY NEURONS

BY MICHAEL J. SHUSTER*, JOSEPH S. CAMARDO† AND STEVEN A. SIEGELBAUM‡

From the Center for Neurobiology and Behavior, Department of Pharmacology, Howard Hughes Medical Institute, Columbia University, 772 West 168th Street, New York, NY 10032, USA

(*Received 7 August 1990*)

SUMMARY

1. Single potassium channel currents were recorded in cell-attached and cell-free patches from *Aplysia* sensory neurons. Two prominent classes of K^+ channels were identified that have similar single-channel current amplitude at 0 mV: (1) the resting conductance serotonin-sensitive K^+ channels (S-channels) previously described in these neurons; and (2) a calcium-activated K^+ channel. A series of experiments were carried out which enable these channels to be distinguished on the basis of their biophysical properties. These experiments also provide further insight into the gating and ionic selectivity of the S-channel.

2. In inside-out patches, single calcium-activated K^+ channel currents ($I_{K,Ca}$) show a linear i–V curve with a slope conductance of 66 pS (normal sea water outside, 360 mM-KCl inside) whereas single S-channels display an outwardly rectifying i–V curve with a slope conductance of 90 pS at 0 mV.

3. The gating of $I_{K,Ca}$ has a steep voltage dependence, with open probability showing an e-fold increase for a 16 mV depolarization. Increasing internal calcium concentration from 0·2 to 10 μM shifts the activation curve by 60 mV in the hyperpolarizing direction.

4. S-channel gating is independent of internal calcium (from < 10 nM up to 100 μM). Steady-state open probability of the S-channel generally shows a weak dependence on membrane potential, with open probability increasing twofold for a 30–100 mV depolarization. Occasional patches were observed with S-channels displaying a much greater voltage sensitivity, with open probability increasing e-fold for a 16–20 mV depolarization.

5. S-channels are selective for K^+ over Na^+. The selectivity ratio depends on the ratio of Na^+ to K^+ concentration on the same side of the membrane. Increasing K^+ concentration appears to increase relative Na^+ permeability, suggesting ion–ion interactions within the channel.

* Present address: Department of Biochemistry and Biophysics, University of California, San Francisco, CA 94143-0448, USA.

† Present address: Wyeth-Ayerst Research, P.O. Box 8299, Philadelphia, PA 19101, USA.

‡ To whom correspondence should be sent.

MS 8708

6. We conclude that *Aplysia* sensory neurons contain two prominent distinguishable classes of K^+ channels, the Ca^{2+}-independent S-channel and a Ca^{2+}-activated channel. The gating properties of the S-channels allow them to contribute outward repolarizing current over a wide range of membrane potentials so that their modulation by neurotransmitters contributes to changes in both resting potential and action potential duration.

INTRODUCTION

Excitable and non-excitable cells contain a variety of K^+ channels which share the property of selectively conducting K^+ ions across cell membranes (Aldrich & Thompson, 1980; Hille, 1984; Rudy, 1988). Yet despite this similarity, different types of K^+ channels differ markedly in their K^+ selectivity, single-channel conductance, and in the influence of membrane potential, intracellular Ca^{2+} activity, and other second messengers on channel gating. Such differences in K^+ channel properties reflect the diverse roles that these channels play in determining cell resting and action potentials.

In *Aplysia* sensory neurons, 5-HT (5-hydroxytryptamine or serotonin) decreases a resting potassium current termed the S-current (for serotonin-sensitive) via cyclic AMP-dependent phosphorylation (Klein, Camardo & Kandel, 1982; Pollock, Bernier & Camardo, 1985; Baxter & Byrne, 1989). Using single-channel recording, a resting K^+ channel was identified that is closed by 5-HT in an all-or-none manner (Siegelbaum, Camardo & Kandel, 1982; Brezina, Eckert & Erxleben, 1987; Pollock & Camardo, 1987) through cyclic AMP-dependent phosphorylation (Shuster, Camado, Siegelbaum & Kandel, 1985). These studies have shown that the S-channel is active at the resting potential, shows only weak voltage-dependent gating, and displays an outwardly rectifying single-channel current–voltage relation (Siegelbaum *et al.* 1982). The S-channel is also relatively insensitive to the K^+ channel blockers tetraethylammonium (TEA) and 4-aminopyridine (4-AP) (Klein *et al.* 1982; Shuster & Siegelbaum, 1987; Baxter & Byrne, 1989). Closure of the S-channel by 5-HT is thought to contribute to a slow depolarization and increase in action potential duration in the sensory neurons. In contrast to the action of 5-HT, the neuropeptide FMRFamide (Phe-Met-Arg-Phe-NH_2) increases the activity of the S-channel (Belardetti, Kandel & Siegelbaum, 1987; Brezina *et al.* 1987) by increasing channel open probability through 12-lipoxygenase metabolites of arachidonic acid (Piomelli, Volterra, Dale, Siegelbaum, Kandel, Schwartz & Belardetti, 1987; Belardetti, Campbell, Falck, Demontis & Rosolowsky, 1989; Buttner, Siegelbaum & Volterra, 1989). The increase in S-channel opening hyperpolarizes the sensory neuron and decreases action potential duration.

Recently, it has become clear that the actions of 5-HT on macroscopic currents in the sensory neuron are more complex than originally reported. Thus, in pleural sensory neurons, 5-HT also decreases a calcium-activated K^+ current (Walsh & Byrne, 1989), alters the kinetics of a voltage-dependent delayed rectifier K^+ current in a cyclic AMP-independent manner (Baxter & Byrne, 1989), and increases an L-type calcium current (Edmonds, Klein, Dale & Kandel, 1990). Finally, despite the overall similarities between the macroscopic S-current and single S-channel recordings, the macroscopic serotonin-sensitive current is more voltage dependent

(Klein *et al.* 1982; Baxter & Byrne, 1989) than single S-channel currents (Siegelbaum *et al.* 1982; Brezina *et al.* 1987; Pollock & Camardo, 1987).

The above findings prompted us to examine in more detail the biophysical properties of the S-channel to address the following questions. Is the S-channel truly distinct from the calcium-activated K^+ channels? To what extent does S-channel gating depend on voltage? How selective is the S-channel for potassium over sodium? Our results show that S-channel gating is independent of internal Ca^{2+} and can be further distinguished from the calcium-activated K^+ channel by its outwardly rectifying single-channel i–V relation. While S-channel gating is usually only weakly dependent on membrane potential, we now show that the channels can exhibit a more strongly voltage-dependent gating behaviour. Finally, we also show that the S-channel is highly selective for potassium over sodium.

METHODS

Preparation and patch-clamp recordings

S-channel currents were recorded from cell-attached, inside-out and outside-out membrane patches (Hamill, Marty, Neher, Sakmann & Sigworth, 1981) from *Aplysia* abdominal ganglion sensory neurons with a List EPC5 patch clamp as previously described (Shuster & Siegelbaum, 1987). All experiments were performed at room temperature (20–25 °C).

Solutions

The artificial sea water (ASW) contained (mM): 460 NaCl, 55 $MgCl_2$, 11 $CaCl_2$, 10 KCl, 10 Tris buffer, pH 7·6. In most experiments with inside-out patches, the electrode was filled with artificial sea water and the bath contained an intracellular-like high-K^+, low-Ca^{2+} solution composed of (mM): 10 NaCl, 2 $MgCl_2$, 1 $CaCl_2$, 360 KCl, 10 K-HEPES buffer, 1·5 EGTA, 272 sucrose, pH 7·4 (internal medium). The [free Ca^{2+}] was estimated to be 200 nM using the affinity constants of Ca^{2+}, Mg^{2+}, and H^+ for EGTA given in Bjerrum, Schwarzenbach & Sillen, (1957), including a correction for ionic strength (Martell & Smith, 1974). For recordings with outside-out patches, electrodes were usually filled with the high-K^+ intracellular medium.

Data analysis

Voltage-dependent gating. The voltage dependence of S-channel gating was studied in cell-attached, inside-out and outside-out cell-free patches. For experiments with the attached and inside-out patches, the electrodes usually were filled with ASW. In several experiments using these patch orientations, the electrodes were filled with the high-K^+ intracellular medium to measure inward S-channel currents at hyperpolarized potentials. For experiments with outside-out patches, the electrodes were filled either with intracellular medium (1 mM-Ca^{2+}, 1·5 mM-EGTA; [free Ca^{2+}] $\sim$ 0·2 μM), or with 0 mM-Ca^{2+}, 10 mM-EGTA intracellular medium, ([free Ca^{2+}] $<$ 10 nM). The bath was superfused with ASW for experiments with cell-attached and outside-out patches, and with intracellular medium for experiments with inside-out patches.

Two protocols were used to study the voltage dependence of S-channel gating. Steady-state measurements of channel open probabilities were determined using current recordings that lasted from 10 s to 2 min, at a fixed membrane potential. The currents were low-pass filtered at 1 kHz, stored on magnetic tape, and later digitized for analysis using an LSI 11-23 laboratory computer. For kinetic analysis of channel gating, the membrane potential was stepped from a steady holding potential to a test potential, and currents either were sampled at 1 kHz, digitized and stored directly on disc, or were filtered at 1 kHz and stored on magnetic tape. The taped data were later digitized for computer analysis. The mean current $\bar{I}$, flowing through a population of channels, is given by:

$$\bar{I} = Npi, \tag{1}$$

where N is the number of channels, i is the current flow through a single open channel, and p is the probability that a single channel is open. In our experiments, $\bar{I}$ was obtained by integrating the

current record and dividing the integral by the duration of the record and i was measured directly. Np was determined in two ways. In the first method, Np was obtained from the ratio $\bar{I}/i$. In the second method, Np was determined from the following expression:

$$Np = \sum_{j=0}^{j_{max}} p(j)j, \tag{2}$$

where $p(j)$ is the probability of observing j channels open simultaneously and j_{max} is the maximum number of channels open simultaneously. $p(j)$ was calculated from the fraction of time that the patch current record spent at the jth level. In all experiments, a binomial distribution was fitted to the observed distributions of channel openings using the method of maximum likelihood (Patlak & Horn, 1982) to determine N, the number of channels in the patch, and p, the single-channel open probability. In patches where channels were in similar gating modes (see below), the data were well fitted by the binomial distribution. However, the product Np could only be reliably separated into its components in those patches where p was relatively large. Therefore, for most of these analyses we have used the product Np to characterize channel gating. Assuming that N does not change with voltage, this still allows the determination of the relative effects of voltage on gating.

Single-channel current–voltage relations. S-channel i–V curves were fitted by the following Goldman–Hodgkin–Katz (GHK) current equation (Hodgkin & Katz, 1949),

$$i_K = \frac{P_K F^2 V([K^+]_i - [K^+]_o \exp(-FV/RT))}{RT(1-\exp(-FV/RT))}, \tag{3}$$

using a non-linear least-squares method to obtain estimates for P_K, the single-channel K^+ permeability. F, V, R and T have their usual meanings. In some cases, a modified version of this equation was used to allow for some sodium permeability. In these cases, single-channel currents were fitted by the sum of two terms for the contributions of K^+ and Na^+ (i.e. $i_S = i_K + i_{Na}$), using eqn (3) and a variable ratio of P_{Na}/P_K.

Selectivity measurements. Ion-selectivity experiments were performed using the high-KCl intracellular medium (see above) in the pipette. Current–voltage curves were measured first under symmetrical ionic conditions with intracellular medium in the bath. The bath next was superfused with intracellular medium in which some of the K^+ was substituted with Na^+. Liquid junction potentials resulting from the ion substitutions accompanying solution changes were less than 1 mV. Polarization between the patch electrode and the ground electrode was monitored periodically by remeasuring the S-channel reversal potential with intracellular medium in the bath (i.e. 0 mV). Corrections for these drifts were applied as necessary. Reported potentials are given as the inside potential (at the cytoplasmic surface of the membrane) minus the external potential, with no correction for the small liquid junction potential. The currents were filtered at 1 kHz, stored on magnetic tape using an FM tape-recorder and were later replayed onto a Gould Brush chart-recorder for analysis by hand of single-channel current amplitudes. Reversal potentials for channel currents were estimated from plots of the current–voltage curves. Shifts in reversal potential resulting from ion substitution were translated into permeability ratios for K^+ and Na^+ using the GHK equation for reversal potential E_r:

$$E_r = \frac{RT}{F} \ln \frac{P_K[K^+]_o + P_{Na}[Na^+]_o}{P_K[K^+]_i + P_{Na}[Na^+]_i} \tag{4}$$

(Hodgkin & Katz, 1949). In this analysis we have assumed that Mg^{2+} and Ca^{2+} have little effect on reversal-potential measurements since the concentration of these divalent cations is quite low. In addition, we have assumed that the channel shows no Cl^- permeability (see Pollock, 1985). The permeability ratio for K^+ and Na^+ was determined in seven inside-out patches and two outside-out patches. For two experiments with inside-out patches, and for one experiment with the outside-out patch, the electrodes were filled with intracellular medium containing 360 mM-KCl and 10 mM-NaCl. For the remaining five experiments with inside-out patches, and the second experiment with the outside-out patch, the electrodes were filled with a modified intracellular medium containing 360 mM-KCl and 0 mM-NaCl. The inclusion of 10 mM-NaCl in the pipette solution had no measurable effect on S-channel selectivity, or single-channel conductance. However, higher

concentrations of Na^+ on either side of the membrane produce partial blockade of channel currents (see below).

RESULTS

The S-channel can be distinguished from the calcium-activated K^+ channel

Single-channel recordings from *Aplysia* sensory neurons reveal two major classes of K^+ channels with similar single-channel current amplitudes but very different sensitivities to intracellular calcium (Fig. 1). One type of channel is active in relatively low internal calcium and shows, in general, gating that is only weakly dependent on membrane voltage (although see below). Fig. 1*A* shows an example of a patch containing one of these calcium- and voltage-insensitive channels. The channel open probability was equal to 0·8 at −30, 0 or +60 mV (internal calcium was 0·2 μM). The channel current–voltage relation shows outward rectification and can be fitted by the GHK constant field current equation (eqn (3)) (Fig. 1*D*), yielding a value for single-channel K^+ permeability (P_K) of $1{\cdot}0 \times 10^{-13}$ cm³/s. This channel is identified as an S-channel, based on its voltage-insensitive gating, calcium-independence, and single-channel *i–V* curve which yields a value for P_K nearly identical to the value of $0{\cdot}9 \times 10^{-13}$ cm³/s originally obtained for S-channels closed by 5-HT in cell-attached patches (Siegelbaum *et al.* 1982).

In contrast to the behaviour of the S channel, the second class of K^+ channels we observe behave as typical calcium-activated K^+ channels (Marty, 1983). Thus, these channels are very sensitive to intracellular calcium concentration and exhibit voltage-dependent gating (Fig. 1*B* and *C*). Figure 1*B* shows records from a patch that contained a single calcium-activated K^+ channel. In the presence of 0·2 μM-Ca^{2+}, this channel was closed. Upon elevating internal calcium to 4·3 μM, the channel opens in a voltage-dependent manner. Upon depolarizing the membrane from −30 mV to +60 mV, there is an increase in channel open probability from 0·15 to 0·52.

In contrast to the S-channel, the calcium-activated K^+ channel exhibits a linear current–voltage relation. In inside-out patches with 360 mM-KCl in the bath, the calcium-activated K^+ channel displays an average conductance of 59·9 ± 6·6 pS (mean ± S.D., $n = 12$) whereas the average slope conductance of the S-channels at 0 mV is 89·1 ± 13·5 pS ($n = 14$).

The similarity in single-channel current amplitudes of these two channels raises the question as to whether these are indeed distinct channels or whether they represent a single type of channel, whose properties are influenced by patch conformation. For example, might calcium-independent S-type channel gating arise as an artifactual behaviour of calcium-activated K^+ channels in inside-out patches where there is poor access of the patch to the bath solution? The experiment shown in Fig. 1*C* makes such possibilities unlikely since the gating of a single S-type channel and a single calcium-activated channel can be clearly distinguished in the same patch. In the presence of 200 nM-free Ca^{2+}, only a single S-type channel is active (the channel shown in Fig. 1*A* and *D*). Upon raising internal calcium to 100 μM, a second K^+ channel is activated (Fig. 1*Ca*). The calcium-activated K^+ channel has a somewhat smaller single-channel current amplitude than the S-channel. This is even more evident at positive potentials and allows the contributions of the two channels to be unambiguously identified (Fig. 1*Cb*).

The voltage and calcium sensitivity of the *Aplysia* calcium-activated K^+ channel are similar to those described for the B-K-type calcium-activated K^+ channel in vertebrates (Marty, 1983). Like those channels (Blatz & Magleby, 1984; Yellen, 1984), the *Aplysia* sensory neuron channel is also very sensitive to external TEA,

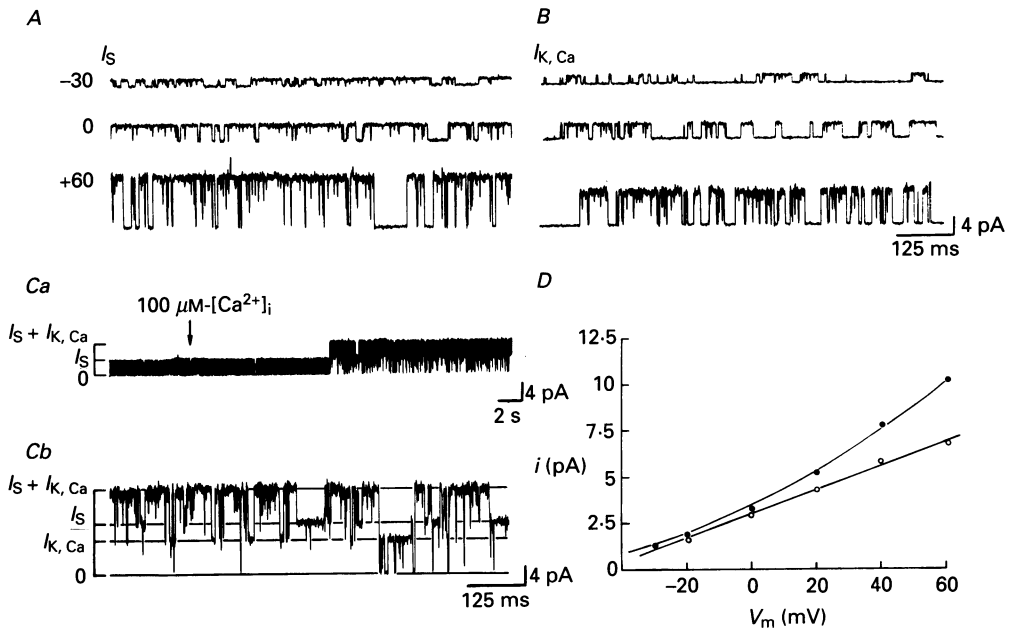

Fig. 1. Distinct single Ca^{2+}-activated K^+ channel currents ($I_{K,Ca}$) and S-channel currents (I_S). *A*, S-channel gating is voltage independent. Records from inside-out patch with a bath free-calcium concentration of 0·2 μM. Channel open probability is 0·8 at all three potentials. *B*, Ca^{2+}-activated channel is voltage dependent. Single Ca^{2+}-activated K^+ channel recorded in an inside-out patch with bath calcium concentration of 4·3 μM. In 0·2 μM-Ca^{2+} no channel openings were observed at the same potentials. Channel open probability was 0·15 at −30 mV, 0·38 at 0 mV, and 0·52 at +60 mV. *C*, recordings showing I_S and $I_{K,Ca}$ activity in same patch. *Ca*, with 0·2 μM-Ca^{2+} in bath, only the S-channel opens. At arrow, bath Ca^{2+} concentration was raised to 100 μM. After 10 s (due to slow perfusion), the Ca^{2+}-activated K^+ channel starts to open. Membrane potential was 0 mV. *Cb*, expanded sweep in 100 μM-Ca^{2+} at a membrane potential of +60 mV showing the two channels active. At this voltage, single S-channel currents are about 30% larger than single Ca^{2+}-activated K^+ currents (*D*), allowing the two channels to be distinguished. *D*, single channel *i–V* plot for the S-current (●) obtained in 0·2 μM-free Ca^{2+}. V_m is the membrane potential. Fitted curve is eqn (3) with a K^+ permeability of $1{\cdot}0 \times 10^{-13}$ cm^3/s and a P_{Na}/P_K ratio of 0·05. ○, Ca^{2+}-activated K^+ channel *i-V* curve measured in intracellular medium containing 100 μM-free Ca^{2+}. Straight line fitted to $I_{K,Ca}$ data by linear regression yields a conductance of 66 pS. Records filtered at 1 kHz in *A*, *B*, and *Cb* and 250 Hz in *Ca*.

with an effective dissociation constant (K_D) of around 0·3 mM (M. J. Shuster and S. A. Siegelbaum, unpublished observations). The major difference is that the single-channel conductance of the *Aplysia* channel is severalfold less than the vertebrate channel.

We next investigate the effect of voltage and calcium on the gating of the calcium-activated and S-channels in more detail. Our goal here is not to present a detailed characterization of the calcium-activated K^+ channel but, rather, to provide further quantitative data that allow us to distinguish this channel from the S-channel.

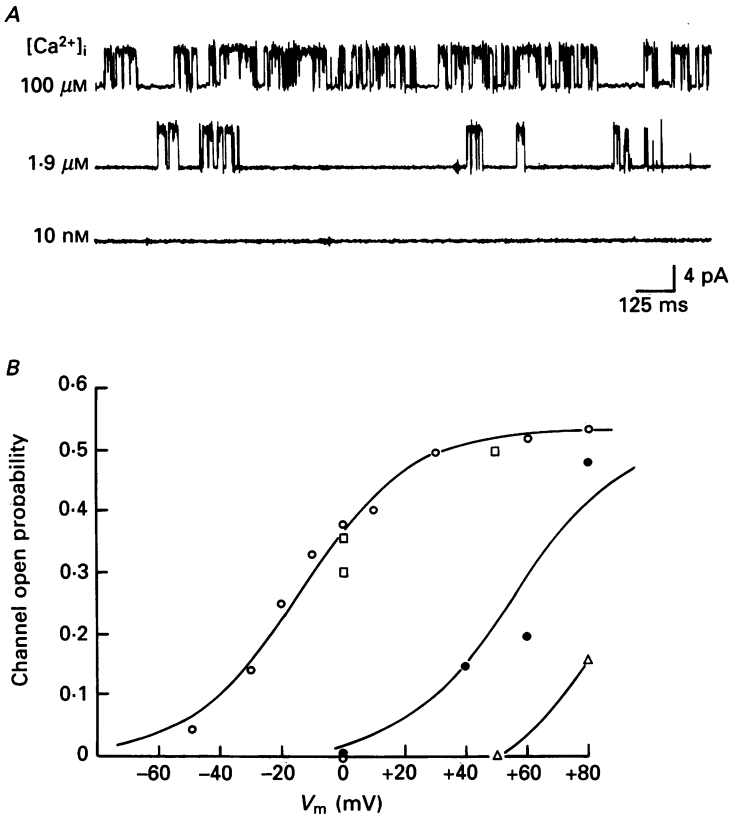

Fig. 2. Gating of the Ca^{2+}-activated K^+ channel depends on $[Ca^{2+}]_i$ and voltage. *A*, single-channel currents from an inside-out patch with a single Ca^{2+}-activated K^+ channel. Membrane potential, $V_m = +60$ mV. $[Ca^{2+}]_i = 100$ μM, top trace; 1·9 μM, middle trace; 10 nM, bottom trace. *B*, dependence of channel open probability on membrane voltage and $[Ca^{2+}]_i$. $[Ca^{2+}]_i$ were (μM): 100 (□), 4·3 (○), 1·9 (●), 1·3 (△). Channel open probabilities measured from 32 s of data. Smooth curves are Hodgkin–Huxley activation curves with slope (s) of 16 mV per e-fold change and mid-points of activation (V_h) at +50 mV for $[Ca^{2+}]_i = 1·9$ μM and −17 mV for $[Ca^{2+}]_i = 4·3$ μM. Maximal channel open probability = 0·53 in this experiment.

The effects of calcium and voltage on the gating of a single calcium-activated K^+ channel are shown in Fig. 2. Raising internal calcium, at a fixed membrane potential, leads to a marked increase in channel open probability (Fig. 2*A*). As found in other preparations, calcium appears to increase channel opening by shifting the voltage dependence of gating to more negative potentials (e.g. Barrett, Magleby & Pallotta,

1982). In this experiment, raising calcium to 4·3 μM apparently shifts the curve maximally since the curves at 4·3 μM- and 100 μM-free Ca^{2+} are identical. A more quantitative analysis of this channel is hampered by significant variability in the sensitivity of the channel to calcium among different patches.

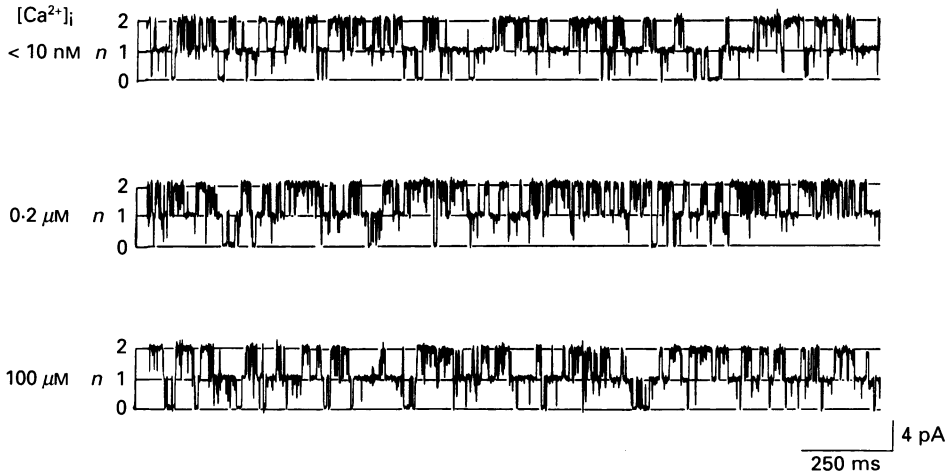

Fig. 3. Gating of the S-channel is insensitive to $[Ca^{2+}]_i$. Currents from an inside-out patch with two channels, in the presence of intracellular medium containing $[Ca^{2+}]_i$ of < 10 nM (top sweep), 0·2 μM (middle sweep), and 100 μM. V_m = 0 mV throughout; n is the number of channels open. Channel open probabilities were measured from 16 s stretches of data at each $[Ca^{2+}]_i$. Open probability is 0·65 with < 10 nM-$[Ca^{2+}]_i$, 0·70 with 0·2 μM-$[Ca^{2+}]_i$, and 0·68 with 100 μM-$[Ca^{2+}]_i$. Current records filtered at 1 kHz.

In comparison, the insensitivity of S-channel gating to $[Ca^{2+}]_i$ is more fully shown in Fig. 3 for an inside-out patch with two active S-channels. The probability of channel opening is unaffected when $[Ca^{2+}]_i$ is varied from < 10 nM up to 100 μM. This result has been consistently obtained in over twenty patches and applies to channels in both high and low open probability gating modes (see below).

The differences in i–V curves, slope conductance, and gating properties between the S-channel and the Ca^{2+}-activated K^+ channel provide a way to distinguish the two channels, and allow the S-channel to be studied in isolation by keeping the Ca^{2+} concentration at the membrane surface at or below 0·2 μM in cell-free patches. In the rest of this paper, we summarize the results of a series of experiments which characterize in greater detail the gating behaviour and ion selectivity of the S-channel in cell-free membrane patches under such conditions where contributions from calcium-activated K^+ channels are minimized.

Non-stationary gating of S-channels in cell-free membrane patches

Previous experiments on S-channels in cell-attached membrane patches demonstrated non-stationary gating, characterized by spontaneous transitions between high steady-state open probability ($p > 0·5$) and low open probability ($p < 0·1$) gating modes (Siegelbaum *et al.* 1982). In general, the channel switches irreversibly

from the low to the high open probability mode. One question is whether such behaviour is an intrinsic property of the channel or reflects control of channel activity through cellular metabolic processes. Figure 4 shows that the same modal gating switches occur in cell-free membrane patches that lack high-energy

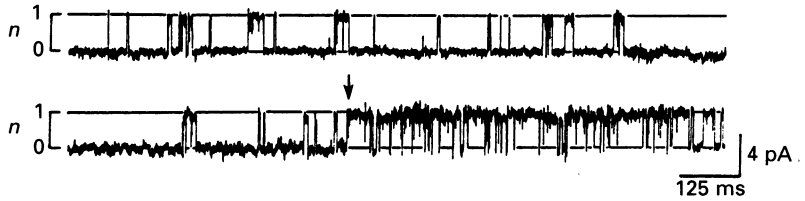

Fig. 4. Non-stationary gating of S-channel in an inside-out patch; n is the number of channels open. Top and bottom traces are continuous in time. Arrow in bottom trace marks transition of channel to high probability mode. Channel open probability was 0·35 before the switch, and 0·78 after it. Probabilities estimated from 12 s stretches of data. Membrane potential held at 0 mV. Current records filtered at 1 kHz.

nucleotides. In this example, the channel showed an abrupt transition from a low to a high open probability mode shortly after the membrane patch was isolated from the cell. Occasionally, such transitions occurred several minutes after patch isolation. Abrupt switches from high to low open probability also occurred, but less frequently than low to high open probability transitions.

Voltage dependence of S-channel gating

One major question concerning S-channel behaviour is the degree to which its gating is voltage dependent. Previous results (Siegelbaum, *et al.* 1982; Camardo, Shuster, Siegelbaum & Kandel, 1983; Brezina *et al.* 1987; Pollock & Camardo, 1987) and the results of Fig. 1 clearly show that under certain conditions, S-channel gating is relatively voltage insensitive. However, examination of a large number of patches shows a wider range in its voltage dependence of gating.

An example of a patch exhibiting a relatively steep voltage dependence of S-channel gating is shown in Fig. 5. The records are from an outside-out patch that contained at least four S-channels. At 0 mV the channels show a relatively low probability of being open ($p < 0{\cdot}1$) and open probability increases markedly as the membrane is depolarized. Figure 5*B* shows a plot of Np as a function of voltage. The superimposed curve shows the best-fit Hodgkin–Huxley gating curve with a slope corresponding to a maximal e-fold change in open probability for a 17·2 mV change in voltage. These channels have been identified as S-channels based on their outwardly rectifying i–V curve (compare with Fig. 1*D*) (fitted by eqn (3) with a value for P_K of $1{\cdot}1 \times 10^{-13}$ cm^3/s). It is highly unlikely that the channels are calcium-activated K^+ channels since the pipette contained a low-calcium solution ([free Ca^{2+}] = 200 nM) and the channels were relatively insensitive to block with 100 mM-external TEA (data not shown). Calcium-activated K^+ channels show nearly complete block with 5–10 mM-TEA.

Between the extremes of channel gating illustrated in Figs 1 and 5, most S-channels display a more moderate degree of voltage-dependent gating. Figure 6 shows an example of such behaviour from an inside-out patch containing a single active S-channel. The channel has an open probability of about 0·50 at 0 mV. As the

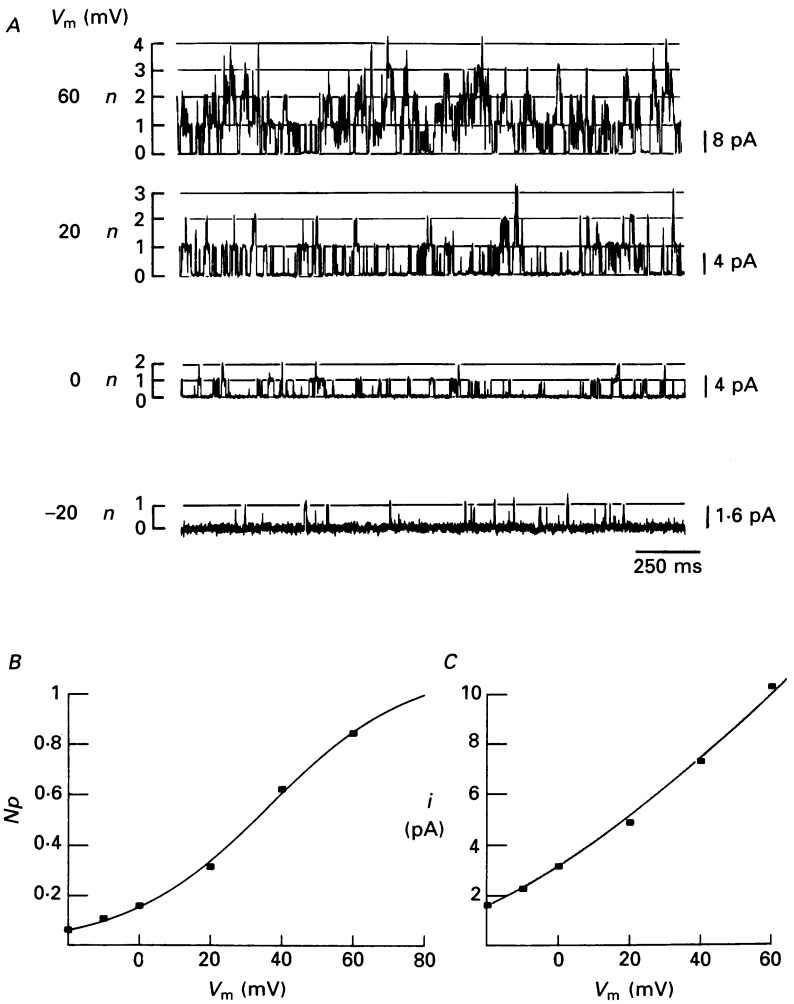

Fig. 5. Steady-state voltage dependence of S-channel gating. Example of strongly voltage-dependent gating. *A*, single-channel current records from outside-out patch at four membrane potentials ranging from −30 to +50 mV. Left-hand ordinate *n*, shows current level associated with zero to four open channels. Note the increase in channel openings with increasing depolarization. Current records filtered at 1 kHz. *B*, steady-state voltage dependence of the open probability, *p*. *Np* obtained from $\bar{I}/i$. $\bar{I}$ measured by averaging 150 s stretches of data at each potential. Curve is linear least-squares best fit of Hodgkin–Huxley gating variable with $V_h = +35$ mV and $s = 17{\cdot}2$ mV. *C*, plot of single-channel current–voltage curve. Continuous line is fit of eqn (3) to data using a P_K value of $1{\cdot}1 \times 10^{-13}$ cm^3/s and $P_{Na}/P_K = 0{\cdot}1$.

membrane potential across the patch is depolarized to +60 mV, the open probability increases to 0·73. Conversely, as the patch is hyperpolarized to −40 mV, the channel open probability decreases to 0·37, corresponding to a twofold increase in open probability for a 100 mV depolarization.

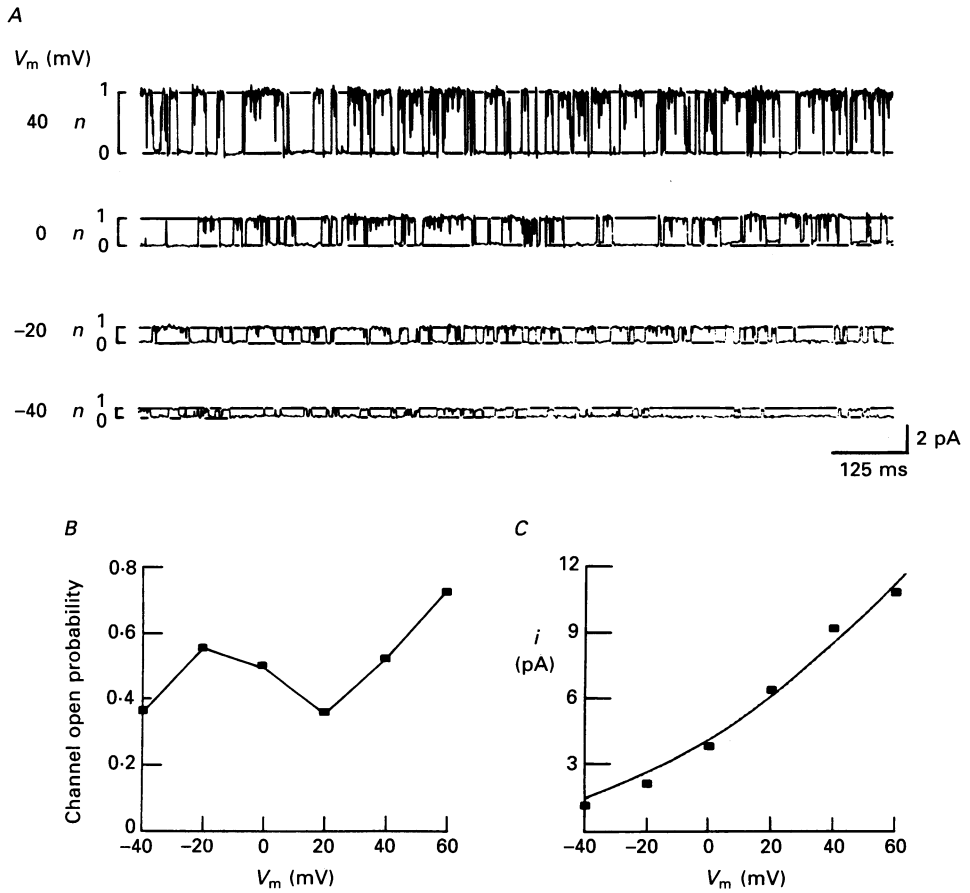

Fig. 6. Steady-state voltage dependence of S-channel gating. Example of moderately voltage-dependent gating. *A*, single-channel current records from an inside-out patch measured at four membrane potentials ranging from −40 to +40 mV. Left-hand ordinate *n*, shows current level associated with open channel ($n = 1$). Note the slight increase in open probability as membrane is depolarized. Current records filtered at 1 kHz. *B*, channel open probability determined from 30 s stretches of data. Gating of channel is only slightly voltage dependent, and shows a maximal slope in the activation curve of approximately 100 mV for a twofold change in open probability over the range from −40 to +60 mV. *C*, plot of single-channel current–voltage relation. Continuous line is fit of eqn (3) to data using a P_K of $1{\cdot}2 \times 10^{-13}$ cm^3/s.

The above results show that there is significant variability in both S-channel open probability and voltage dependence of gating. To summarize this variability in gating behaviour we have plotted, for each patch, channel voltage dependence as a

function of open probability (measured at 0 mV; Fig. 7). Since it was not generally possible to quantify voltage dependence by fitting Boltzmann gating curves to the data, we obtained an approximate measure of voltage dependence by measuring the maximum slope of the relationship between open probability and voltage, expressed

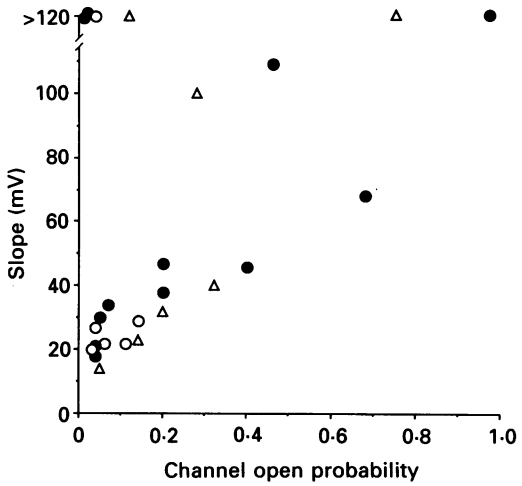

Fig. 7. Comparison of S-channel voltage dependence with open probability for cell-attached (△), inside-out (●) and outside-out (○) patches. For each patch, maximal voltage dependence was measured by fitting a straight line to open probability *vs.* voltage plots and measuring the slope of the line in terms of the depolarization required to increase open probability (at steepest point) by a factor of two. Voltage dependence plotted as function of open probability at 0 mV. Each point is a separate patch.

as the number of millivolts of depolarization required for a twofold increase in open probability. The data of Fig. 7 show that S-channels in outside-out patches tend to exhibit more voltage dependence than channels in either inside-out or cell-attached patches. Thus, in five out of six outside-out patches, S-channel gating required a depolarization of only 30 mV or less for a twofold increase in opening. In contrast, S-channels in inside-out patches and cell-attached patches showed a similar extent of voltage-dependence in only two out of twelve patches and two out of seven patches, respectively. The data of Fig. 7 also show some correlation between open probability at 0 mV and voltage dependence; channels exhibiting a low open probability often (but not always) showed more steeply voltage-dependent gating.

Ensemble analysis of S-channel gating

While our results show that S-channels can display significant voltage dependence, most channels exhibit a relatively weak voltage dependence that is less than that observed during macroscopic voltage clamp experiments. One possible reason for the discrepancy between macroscopic and microscopic gating lies in the experimental protocol. Macroscopic currents were generally measured using relatively short (200–500 ms) depolarizing clamp pulses whereas single-channel measurements were done using long steady-state depolarizations. Therefore, we have measured S-

channel gating during 200 ms depolarizing voltage clamp pulses from a negative holding potential using ensemble averages. Figure 8 shows a result from such an experiment using the cell-attached patch configuration. The membrane potential across the patch was held at the cell's resting potential (−50 mV), and was

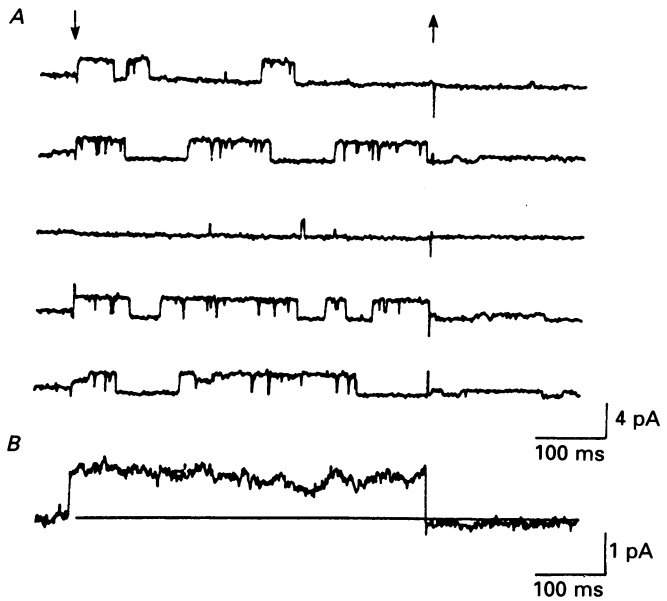

Fig. 8. S-channel gating during voltage jumps. *A*, single S-channel currents from a cell-attached patch in response to depolarizing voltage clamp steps. The five current traces show responses to successive identical 500 ms clamp pulses. The membrane potential was held at the cell resting potential (−50 mV) and depolarized by +50 mV to approximately 0 mV. Note channel openings occur before, during and after the depolarization. The arrows mark the start and end of the pulse. *B*, ensemble-averaged current from 200 depolarizations. Recording from a cell-attached patch with one S-channel. Current records filtered at 500 Hz and sampled at 1 kHz. Capacity transient and linear leakage current have been subtracted.

depolarized by +50 mV (up to 0 mV) for 500 ms, once every 10 s. Figure 8*A* shows examples of single-channel currents before, during, and after five consecutive depolarizing commands. Channels open throughout the sweep (although the unit current pulses at −50 mV are small), without any obvious correlation with the depolarizing pulse. Figure 8*B* shows the current obtained by averaging 200 jumps to 0 mV. No time-dependent changes are apparent in the average current. This result was consistently obtained in three cell-attached patches. A similar result was obtained with S-channels in inside-out ($n = 3$), and outside-out ($n = 2$) cell-free membrane patches.

These results obtained with S-channels in cell-attached, inside-out, and outside-out membrane patches suggest that the voltage dependence of S-channel gating occurs with a time course that is outside the time resolution of the protocols we have used. The limits of this time resolution are determined by the cut-off frequency at which the records were filtered, and the sample rate at which they were digitized

(500 Hz, and 1 kHz, respectively, to give a minimum time resolution of 2 ms), and by the duration of the voltage steps (several hundred milliseconds). Several possible interpretations of this result are considered in the Discussion.

S-channel selectivity for K^+ vs. Na^+

Although previous single-channel studies have shown that the S-channel is sensitive to internal K^+ concentration (Siegelbaum *et al.* 1982), the extent to which

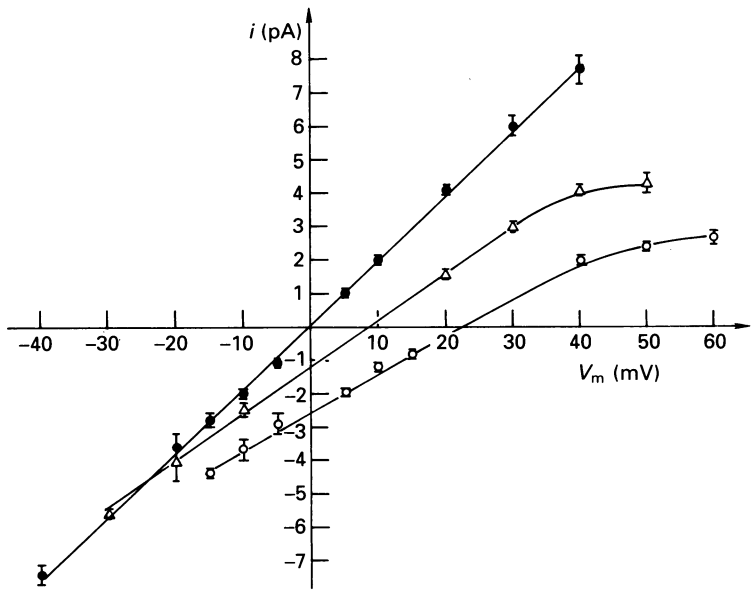

Fig. 9. S-channel reversal potential. Reversal potentials determined with inside-out patch. Patch pipette contained 360 mM-KCl, 0 mM-NaCl. Reversal potentials determined with three bath solutions (mM): 360 KCl, 0 NaCl (●); 240 KCl, 120 NaCl (△); and 120 KCl, 240 NaCl (○) were respectively 0, 8·5 and 22·5 mV. Error bars indicate S.D. These yield estimates for P_{Na}/P_K of 0·14 (240 mM-KCl value) and 0·11 (120 mM-KCl value).

it selects for K^+ relative to Na^+ is not known. To investigate S-channel ionic selectivity we determined S-channel i–V curves with different concentrations of NaCl and KCl in the bathing solutions. Figure 9 shows S-channel i–V curves measured from an inside-out patch with 360 mM-KCl, 0 mM-NaCl in the pipette. The filled circles show the linear i–V curve measured with a 360 mM-KCl solution in the bath. The absence of outward rectification in this i–V curve demonstrates that the rectification that normally is seen results from the asymmetric distribution of K^+ across the membrane under normal ionic conditions. The measured reversal potential under these conditions is 0 mV, as expected. Next, the bath solution was changed to a 240 mM-KCl, 120 mM-NaCl intracellular medium. The i–V curve was remeasured (△), and the reversal potential was shifted to +8·5 mV, yielding a value for P_{Na}/P_K of 0·14. The bath then was superfused with 120 mM-KCl, 240 mM-NaCl, and the i–V curve remeasured (○). Now the single S-channel current reverses at +22·5 mV. This potential gives a permeability ratio of 0·11.

As internal Na^+ is raised, maximal channel slope conductance is reduced and the outward current reaches a saturating value with voltage at lower values of i. In addition, the current record during channel opening becomes noisy (data not shown). These results are consistent with the view that internal Na^+ blocks the open channel in addition to carrying charge through the channel (see Yellen, 1984).

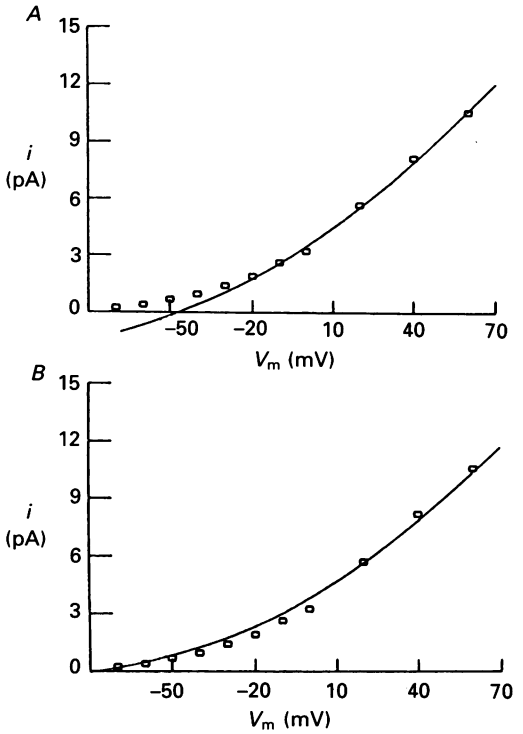

Fig. 10. Fit of single-channel current–voltage relation by eqn (3) over range of membrane potential from −70 to +60 mV. *A*, using a P_{Na} value equal to 0·1 of P_K, eqn (3) fits depolarized end of S-channel current–voltage relation, but predicts a reversal potential of −48 mV, while the channel carries outward current at potentials as hyperpolarized as −70 mV. *B*, fit of same data, using P_{Na} value of 0·013 P_K, obtained from linear extrapolation estimate of the reversal potential for this channel (−79 mV). Fit is improved, but systematic deviations of the data from the curve still occur at hyperpolarized potentials. $P_K = 1{\cdot}15 \times 10^{-13}$ cm³/s for curve plotted in *A*, and $1{\cdot}10 \times 10^{-13}$ cm³/s in *B*.

Table 1 presents the results of nine ion-substitution experiments using both inside-out and outside-out patches. Similar selectivity ratios were obtained with the two patch configurations. The average value for P_{Na}/P_K is $0{\cdot}11 \pm 0{\cdot}06$ (mean ± S.D., n = 17). The range is from 0·01 up to 0·21, with most of the estimates clustering in the range of 0·11 to 0·15. There is a trend toward greater potassium ion selectivity as the potassium ion concentration becomes more asymmetric across the membrane. While this result indicates that K^+ is the major charge carrier for the S-current, a P_{Na}/P_K ratio of 0·1 predicts a reversal potential at around −40 mV for channel currents

measured under the normal ionic conditions of ASW on the outside (460 mM-Na^+, 10 mM-K^+), and normal internal ionic concentrations of 240 mM-K^+, 10 mM-Na^+. This implies that the S-channels will carry inward current at the normal sensory neuron resting potential (around −50 mV) and thus S-channel closure could not contribute to the depolarizing action of serotonin.

TABLE 1. P_{Na}/P_K selectivity ratios

Inside-out patches

$[K^+]_o$, $[Na^+]_o$ (mM)	360,0	360,0	360,0	360,0
$[K^+]_i$, $[Na^+]_i$ (mM)	10,350	40,320	120,240	240,120
	0·10	0·11	0·15	—
	—	0·01	0·014	—
	—	—	0·11	0·14
	—	—	0·11	0·14
	—	—	0·15	—
	—	—	0·01	—

Outside-out patches

$[K^+]_o$, $[Na^+]_o$ (mM)	60,300	120,240	240,120
$[K^+]_i$, $[Na^+]_i$ (mM)	360,0	360,0	360,0
	0·09	0·10	0·21
	—	0·16	0·19

Permeability ratios (P_{Na}/P_K) obtained from S-channel reversal potential measurements in inside-out (top) or outside-out (bottom) patches. Each row represents measurements from a different patch. Na^+ and K^+ concentratiions on both sides of membrane for each measurement indicated in top rows. Experiments where Na^+ concentration is listed as 0 also include data obtained with 10 mM-Na^+.

To resolve this discrepancy, we extended our measurement of the S-channel i–V curve to a more negative range of voltages than normally investigated. These results show that under normal (or near normal) ionic conditions, the S-channels carry outward current at potentials as negative as −70 mV in both cell-attached ($n = 3$) and inside-out cell-free patches ($n = 2$). At more negative voltages, the channel currents are too small to measure accurately. Figure 10 shows an S-channel current–voltage curve measured from an inside-out patch with ASW in the pipette and 360 mM-KCl intracellular medium in the bath. Linear extrapolation of the single-channel current–voltage curve from the hyperpolarized portion of the curve (negative to −40 mV) yields an estimate for the reversal potential of −79 mV, which is equivalent to a P_{Na}/P_K ratio of 0·013. This estimate should be an upper limit on the true ratio since the linear extrapolation probably overestimates the value of the reversal potential. The i–V curve has been fitted with the GHK constant field current equation (eqn (3)) using either a P_{Na}/P_K ratio of 0·1 obtained from the ion substitution experiments (Fig. 10*A*) or with a P_{Na}/P_K ratio of 0·013 obtained from the extrapolated reversal potential (Fig. 10*B*). At membrane potentials more negative than 0 mV, there is a marked deviation of the data from the theoretical i–V curve

based on a P_{Na}/P_K ratio of 0·10, whereas the i–V data are better fitted by eqn (3) using 0·013 for the permeability ratio. However, the experimental current points still fall somewhat below the theoretical curve at potentials below 0 mV. An attempt was made to improve the fit of eqn (3) to S-channel i–V curves from several experiments by varying the P_{Na}/P_K ratio. The best fits over an extended range of membrane potentials were obtained when a small P_{Na} term (1–2% of P_K) was included. However, even in the best fits, data points consistently fell below the GHK curve at hyperpolarized potentials.

DISCUSSION

Comparison of S and Ca^{2+}-activated K^+ channels

The results of the experiments described here distinguish between two types of single K^+ channel currents in *Aplysia* sensory neurons; a calcium-activated K^+ channel and the calcium-independent serotonin-sensitive K^+ channel (S-channel). Although both classes of channels have similar conductances and single-channel amplitudes at potentials near 0 mV, they can be differentiated by the shapes of their single-channel i–V relationships, voltage dependence of gating, and internal-calcium sensitivity. Thus, the calcium-activated K^+ channel requires micromolar internal calcium to activate, has a linear i–V relationship and shows a consistent voltage sensitivity of gating, with open probability increasing e-fold for 16 mV of depolarization. In contrast, the S-channel single-channel i–V relation shows outward rectification that is well fitted by the GHK current equation (eqn (3)) yielding a P_K of about 1×10^{-13} cm^3/s, while S-channel gating is independent of internal calcium concentration (10 nM–100 μM). In general S-channel gating is also much less voltage sensitive than the calcium-activated K^+ channel (although see below). Furthermore the S-channel is relatively insensitive to TEA (K_D around 90 mM; Shuster & Siegelbaum, 1987; Baxter & Byrne, 1989) whereas the calcium-activated K^+ channel is completely blocked by 5–10 mM-TEA. The similarity in single-channel amplitude of the calcium-activated and S-channels (especially at 0 mV) necessitates the use of these other criteria to confirm channel identity.

S-channel gating

The S-channel in cell-free patches shares many features with the macroscopic S-current and with the channel in cell-attached membrane patches. The channels and the macroscopic current both are active at the cell's resting potential (regardless of gating mode), insensitive to intracellular [Ca^{2+}], and do not inactivate with prolonged depolarization. The principal difference between single S-channel properties and the macrosopic S-current resides in the details of their time- and voltage-dependent gating. In general, the macrosopic S-current (I_S) displays a greater extent of time-, and voltage-dependent gating compared to our single S-channel current records (although some of the voltage dependence of I_S results from the outwardly rectifying single S-channel i–V curve).

A quantitative assessment of single S-channel gating is complicated by a marked variability in gating behaviour. One source of variability is the observed switch in gating mode from a state where the channel shows a low probability of being open

to a state where the channel is open for a large fraction of time (see Patlak, Gration & Usherwood, 1979; Nowycky, Fox & Tsien, 1985; Blatz & Magleby, 1986 for other examples of non-stationary gating). Such transitions are generally stable and can persist for tens of minutes or even hours. Within a given gating mode there also can be more subtle variations in open probability on a time scale of minutes, where open probability may fluctuate up and down by a factor of two or three.

A second type of variability is the degree to which S-channel gating is voltage dependent. This ranges from channels that are virtually voltage independent to channels that show a marked voltage sensitivity. In general, most S-channels show an intermediate behaviour where open probability increases e-fold for a 30–100 mV depolarization. This voltage dependence is similar to that of the nicotinic acetylcholine receptor (Magleby & Stevens, 1972) and much less than that of a typical voltage-gated channel.

It is possible that the variability in voltage dependence is related to the different modes of gating. Accordingly, one might expect high open probability gating to be associated with a voltage-independent mode and low open probability gating to be associated with a more voltage-dependent behaviour. In general, this trend is observed, as shown by the data of Fig. 7. However, the correlation is not absolute as we see examples of channels in a low open probability mode that are voltage independent. Channels in outside-out patches tend to show a greater extent of voltage-dependent gating compared to channels in cell-attached patches and inside-out patches. Several previous studies have suggested that inside-out patch formation can influence channel properties (Trautmann & Siegelbaum, 1983; Cachelin, de Peyer, Kokubun & Reuter, 1983).

The molluscan peptide FMRFamide modulates S-channel gating by increasing channel open probability (Belardetti *et al.* 1987; Brezina *et al.* 1987) through a second-messenger system involving lipoxygenase metabolites of arachidonic acid (Piomelli *et al.* 1987). It is possible that some of the variability in channel properties we observe are related to variable basal activation of the arachidonic acid cascade. One interesting possibility is that the arachidonic acid cascade could be activated during patch formation as a result of phospholipase A_2 activation resulting from transient membrane damage. Despite these uncertainties, the reliable conductance properties of the S-channel permit its reliable identification in all gating modes.

So far, we have not observed any time-dependent component to S-channel gating that is comparable to the time-dependent increase in macroscopic S-current measured under voltage clamp. In response to a voltage clamp step depolarization from a holding potential of -50 mV to a test potential of around 0 mV, the macroscopic S-current shows a time-dependent increase during the first 100–200 ms of the step until it reaches a steady-state value approximately twofold larger than its initial value (see Klein *et al.* 1982). 5-HT also reduces the magnitude of an outward tail current which decays with a time constant between 50 and 100 ms upon termination of the depolarizing pulse (M. Klein, personal communication).

There are several possible reasons why we have failed to detect a similar time dependence for S-channel gating. First, none of the channels used for our kinetic analysis might have been in an appropriate gating mode. It is possible that the patch procedure *per se* subtly alters channel gating, favouring a voltage-independent mode

with little time-dependent gating over a mode exhibiting voltage- and time-dependent behaviour. The apparent influence of patch configuration on channel voltage dependence (Fig. 7) provides some support for this. Another possibility is that more than one type of channel contributes to the macroscopic S-current, and that the channels we have characterized are not responsible for the time-dependent gating properties of I_S. Thus, several additional actions of 5-HT on sensory neuron ionic currents have recently been described, including a decrease in a calcium-activated K^+ current (Walsh & Byrne, 1989), modulation of a delayed rectifier current (Baxter & Byrne, 1989), and an increase in a dihydropyridine-sensitive calcium current (Edmonds *et al.* 1990).

Ionic selectivity

A second focus of this paper has been a characterization of the S-channel ionic selectivity. Ion substitution experiments indicate that the channel is highly selective for potassium over sodium under normal ionic conditions (i.e. very steep K^+ and Na^+ gradients). However, we find that the relative permeability for potassium over sodium appears to be a function of K^+ and Na^+ concentration gradients. Our results indicate that as the potassium concentration is increased on one side of the membrane relative to sodium concentration on the same side of the membrane, the relative sodium permeability increases. At a fixed concentration ratio, the relative sodium permeability also appears to increase as the membrane potential is driven further away from the potassium equilibrium potential. Both observations could be explained if the S-channel contained multiple binding sites for Na^+ and K^+. According to such a scheme, the ability of Na^+ to permeate would depend on its being driven through the pore due to electrostatic repulsive forces as a result of a K^+ ion entering the pore after sodium and 'pushing' the sodium through. As the K^+ concentration is raised relative to sodium, the chances of K^+ entering after sodium are increased and so the Na^+ permeability is enhanced. More detailed information about selectivity ratios would be required, however, to attempt a quantitative modelling of this behaviour. Preliminary results using a computer program provided by Peter Hess indicate that a two-site three-barrier model cannot reproduce this behaviour, so the S-channel probably contains at least three ionic binding sites.

Many other channels are also thought to have multiple binding sites for ions including the delayed rectifier K^+ channel (Hodgkin & Keynes, 1955), the inward rectifier K^+ channel (Hagiwara, Miyazaki, Krasne & Ciani, 1977; Hille & Schwarz, 1978), the Na^+ channel from squid axon (Begenisich & Cahalan, 1980), and Ca^{2+} channels in heart (Hess & Tsien, 1984) and skeletal muscle (Almers & McCleskey, 1984), suggesting that a pore which can contain more than one ion may be a common structural motif among many ion channels.

We thank Peter Hess for providing his computer program for modelling ion permeation, Eric Kandel for encouragement in these experiments and Kathrin Hilten for preparing the figures. M.J.S. is presently a Lucile P. Markey Fellow of the Life Sciences Research Foundation. This work was partially supported by grant NS-19569 from the NIH to S.A.S.

REFERENCES

ALDRICH, R. W. & THOMPSON, S. H. (1980). Membrane potassium channels. In *Cell Surface and Neuronal Function* ed. COTMAN, C. W., POSTE, G. & NICOLSON, G. L. North-Holland, Amsterdam. Cell Surface Reviews **6**, 50–85.

ALMERS, W. & MCCLESKEY, E. W. (1984). Non-selective conductance in calcium channels of frog muscle: calcium selectivity in a single-file pore. *Journal of Physiology* **353**, 585–608.

BARRETT, J. N., MAGLEBY K. L. & PALLOTTA, B. S. (1982). Properties of single calcium-activated potassium channels in cultured rat muscle. *Journal of Physiology* **331**, 211–230.

BAXTER, D. A. & BYRNE, J. H. (1989). Serotonergic modulation of two potassium currents in the pleural sensory neurons of *Aplysia*. *Journal of Neurophysiology* **62**, 665–679.

BLATZ, A. L. & MAGLEBY, K. L. (1984). Ion conductance and selectivity of single calcium-activated potassium channels in cultured rat muscle. *Journal of General Physiology* **84**, 1–23.

BLATZ, A. L. & MAGLEBY, K. L. (1986). Quantitative description of three modes of activity of fast chloride channels from rat skeletal muscle. *Journal of Physiology* **378**, 141–174.

BEGENISICH, T. B. & CAHALAN, M. D. (1980). Sodium channel permeation in squid axons. II. Non-independence and current–voltage relations. *Journal of Physiology* **307**, 243–257.

BELARDETTI, F., CAMPBELL, W. B., FALCK, J. R., DEMONTIS, G. & ROSOLOWSKY, M. (1989). Products of heme-catalyzed transformation of the arachidonate derivative 12-HPETE open S-type K^+ channels in *Aplysia*. *Neuron* **3**, 497–505.

BELARDETTI, F., KANDEL, E. R. & SIEGELBAUM, S. A. (1987). Neuronal inhibition by the peptide FMRFamide involves opening of S K^+ channels. *Nature* **325**, 153–156.

BJERRUM, J., SCHWARZENBACH, G. & SILLEN, L. G. (1957). *Stability Constants*, part I; *Organic Ligands*, p. 94. The Chemical Society, London.

BREZINA, V., ECKERT, R. & ERXLEBEN, C. (1987). Modulation of potassium conductances by an endogenous neuropeptide in neurones of *Aplysia californica*. *Journal of Physiology* **388**, 565–595.

BUTTNER, N., SIEGELBAUM, S. A. & VOLTERRA, A. (1989). Direct modulation of *Aplysia* S-K^+ channels by a 12-lipoxygenase metabolite of arachidonic acid. *Nature* **342**, 553–555.

CACHELIN, A. B., DE PEYER, J. E., KOKUBUN, S. & REUTER, H. (1983). Sodium channels in cultured cardiac cells. *Journal of Physiology* **340**, 389–401.

CAMARDO, J. S., SHUSTER, M. J., SIEGELBAUM, S. A. & KANDEL, E. R. (1983). Modulation of a specific potassium channel in sensory neurons of *Aplysia* by serotonin and cAMP-dependent protein phosphorylation. *Cold Spring Harbor Symposia on Quantitative Biology* **48**, 213–220.

EDMONDS, B., KLEIN, M., DALE, N. & KANDEL, E. R. (1990). Contribution of two types of calcium channels to synaptic transmission and plasticity. *Science* **250**, 1142–1147.

HAGIWARA, S., MIYAZAKI, S., KRASNE, S. & CIANI, S. (1977). Anomalous permeabilities of the egg cell membrane of a starfish in K^+-Tl^+ mixtures. *Journal of General Physiology* **70**, 269–281.

HAMILL, O. P., MARTY, A., NEHER, E., SAKMANN, B. & SIGWORTH, F. J. (1981). Improved patch-clamp techniques for high-resolution current recording from cells and cell-free membrane patches. *Pflügers Archiv* **291**, 85–100.

HESS, P. & TSIEN, R. W. (1984). Mechanism of ion permeation through calcium channels. *Nature* **309**, 453–456.

HILLE, B. (1984). *Ionic Channels of Excitable Membranes*, pp. 99–117. Sinauer Associates Inc., Sunderland, MA, USA.

HILLE, B. & SCHWARZ, W. (1978). Potassium channels as multi-ion single-file pores. *Journal of General Physiology* **72**, 409–442.

HODGKIN, A. L. & KATZ, B. (1949). The effect of sodium ions on the electrical activity of the giant axon of the squid. *Journal of Physiology* **108**, 37–77.

HODGKIN, A. L. & KEYNES, R. D. (1955). The potassium permeability of a giant nerve fibre. *Journal of Physiology* **128**, 61–88.

KLEIN, M., CAMARDO, J. & KANDEL, E. R. (1982). Serotonin modulates a specific potassium current in the sensory neurons that show presynaptic facilitation in *Aplysia*. *Proceedings of the National Academy of Sciences of the USA* **79**, 5713–5717.

MAGLEBY, K. L. & STEVENS, C. F. (1972). The effect of voltage on the time course of end-plate currents. *Journal of Physiology* **223**, 151–171.

MARTELL, A. E. & SMITH, R. M. (1974). *Critical Stability Constants*. Plenum Press, London.

MARTY, A. (1983). Ca^{2+}-dependent K^+ channels with large unitary conductance. *Trends in Neurosciences* **6**, 262–265.

NOWYCKY, M. C., FOX, A. P. & TSIEN, R. W. (1985). Long-opening mode of gating of neuronal calcium channels and its promotion by the dihydropyridine calcium agonist Bay K 8644. *Proceedings of the National Academy of Sciences of the USA* **82**, 2178–2182.

PATLAK, J. B., GRATION, K. A. F. & USHERWOOD, P. N. R. (1979). Single glutamate-activated channels in locust muscle. *Nature* **278**, 643–645.

PATLAK, J. & HORN, R. (1982). Effect of *N*-bromoacetamide on single sodium channel currents in excised membrane patches. *Journal of General Physiology* **79**, 333–351.

PIOMELLI, D., VOLTERRA, A., DALE, N., SIEGELBAUM, S. A., KANDEL, E. R., SCHWARTZ, J. H. & BELARDETTI, F. (1987). Lipoxygenase metabolites of arachidonic acid as second messengers for presynaptic inhibition of *Aplysia* sensory cells. *Nature* **328**, 38–43.

POLLOCK, J. D. (1985). Serotonin and cAMP modulate S potassium current in pleural sensory neurons. Ph.D. Thesis, Columbia University.

POLLOCK, J. D. & CAMARDO, J. S. (1987). Regulation of single potassium channels by serotonin in the cell bodies of tail mechanosensory neurons of *Aplysia californica*. *Brain Research* **410**, 367–370.

POLLOCK, J. D., CAMARDO, J. S. & BERNIER, L. (1985). Serotonin and cyclic adenosine 3′5′-monophosphate modulate the S potassium current in tail sensory neurons in the pleural ganglion of *Aplysia*. *Journal of Neuroscience* **5**, 1862–1871.

RUDY, B. (1988). Diversity and ubiquity of K^+ channels. *Neuroscience* **25**, 729–749.

SHUSTER, M. J., CAMARDO, J. S., SIEGELBAUM, S. A. & KANDEL, E. R. (1985). Cyclic AMP-dependent protein kinase closes the serotonin-sensitive K^+ channels of *Aplysia* sensory neurones in cell-free membrane patches. *Nature* **313**, 392–395.

SHUSTER, M. J. & SIEGELBAUM, S. A. (1987). Pharmacological characterization of the serotonin-sensitive potassium channel of *Aplysia* sensory neurons. *Journal of General Physiology* **90**, 587–608.

SIEGELBAUM, S. A., CAMARDO, J. S. & KANDEL, E. R. (1982). Serotonin and cyclic AMP close single K^+ channels in *Aplysia* sensory neurones. *Nature* **299**, 413–417.

TRAUTMANN, A. & SIEGELBAUM, S. A. (1983). The influence of membrane patch isolation on single acetylcholine-channel current in rat myotubes. In *Single Channel Recording*, ed. SAKMANN, B. & NEHER, E., pp. 473–480. Plenum Press, New York.

WALSH, J. P. & BYRNE, J. H. (1989). Modulation of a steady-state Ca^{2+}-activation, K^+ current in tail sensory neurons of *Aplysia*: role of serotonin and cAMP. *Journal of Neurophysiology* **61**, 32–44.

YELLEN, G. (1984). Ionic permeation and blockade in Ca^{2+}-activated K^+ channels of bovine chromaffin cells. *Journal of General Physiology* **84**, 157–186.